Title: Anhydride-functional silane immobilized onto titanium surfaces induces osteoblast cell differentiation and reduces bacterial adhesion and biofilm formation

Short title: TESPSA induces osteoblast differentiation and reduces biofilm formation

Authors names:

Maria Godoy-Gallardo[a,b] maria.godoy.gallardo@upc.edu

Jordi Guillem-Marti[a,b] jordi.guillem.marti@upc.edu

Pablo Sevilla[c] psevilla@euss.es

José M. Manero[a,b] jose.maria.manero@upc.edu

Francisco J. Gil[a,b] francesc.xavier.gil@upc.edu

Daniel Rodriguez[a,b] daniel.rodriguez.rius@upc.edu

Affiliations:

[a] Biomaterials, Biomechanics and Tissue Engineering Group, Department of Materials Science and Metallurgy, Technical University of Catalonia (UPC), ETSEIB, Av. Diagonal 647, 08028-Barcelona, Spain.

[b] Centre for Research in NanoEngineering (CRNE) - UPC, C/ Pascual i Vila 15, 08028-Barcelona, Spain.

[c] Department of Mechanics, Escola Universitària Salesiana de Sarrià (EUSS), C/ Passeig de Sant Bosco, 42, 08017-Barcelona, Spain

Correspondence: Dr. Daniel Rodriguez, Department of Materials Science and Metallurgical Engineering, Technical University of Catalonia (UPC). ETSEIB-UPC, Av. Diagonal 647, 08028-Barcelona, Spain. **E-mail**: daniel.rodriguez.rius [at] upc.edu

Graphical abstract

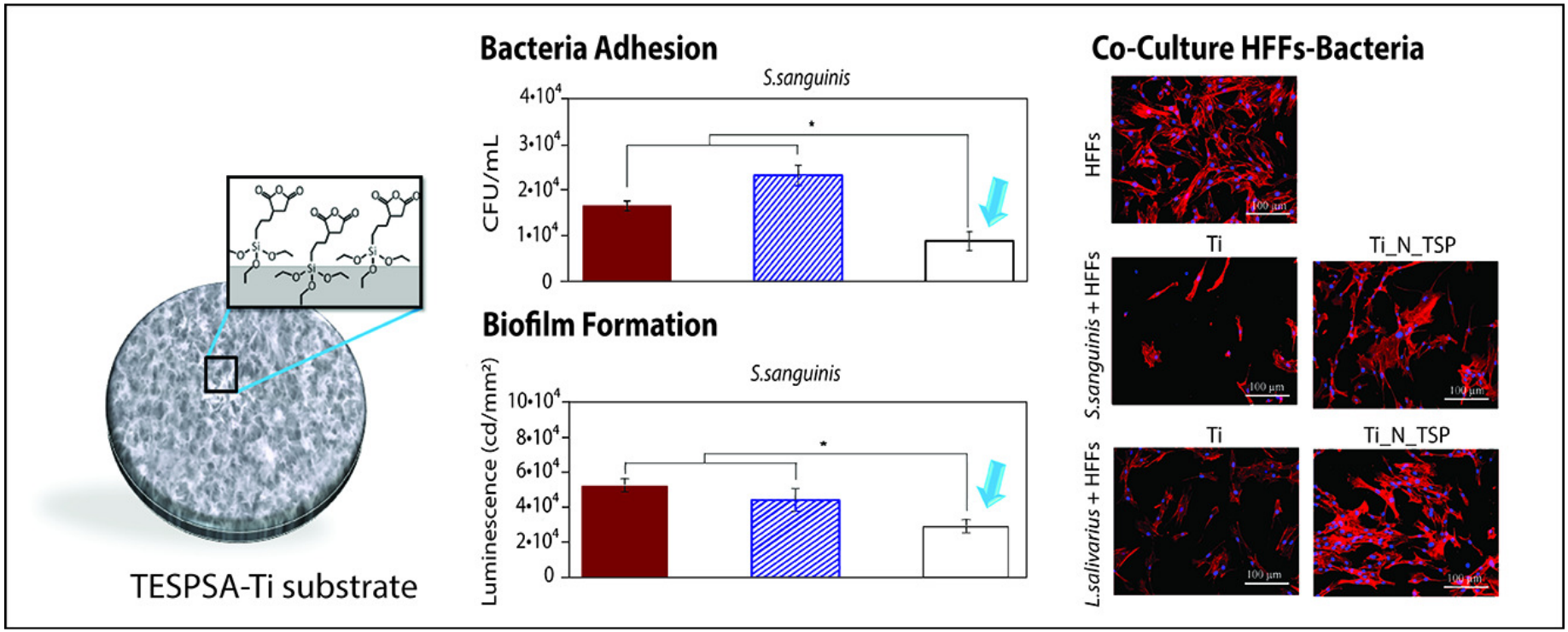

Abstract

Bacterial infection in dental implants along with osseointegration failure usually leads to loss of the device. Bioactive molecules with antibacterial properties can be attached to titanium surfaces with anchoring molecules such as silanes, preventing biofilm formation and improving osseointegration. Properties of silanes as molecular binders have been thoroughly studied, but research on the biological effects of these coatings is scarce. The aim of the present study was to determine the *in vitro* cell response and antibacterial effects of triethoxysilypropyl succinic anhydride (TESPSA) silane anchored on titanium surfaces. X-ray photoelectron spectroscopy confirmed a successful silanization. The silanized surfaces showed no cytotoxic effects. Gene expression analyses of Sarcoma Osteogenic (SaOS-2) osteoblast-like cells cultured on TESPSA silanized surfaces reported a remarkable increase of biochemical markers related to induction of osteoblastic cell differentiation. A manifest decrease of bacterial adhesion and biofilm formation at early stages was observed on treated substrates, while favoring cell adhesion and spreading in bacteria-cell co-cultures.

Surfaces treated with TESPSA could enhance a biological sealing on implant surfaces against bacteria colonization of underlying tissues. Furthermore, it can be an effective anchoring platform of biomolecules on titanium surfaces with improved osteoblastic differentiation and antibacterial properties.

Keywords: bacterial adhesion; biofilm; osteoblast differentiation; silane; titanium

Highlights

- TESPSA silane induces osteoblast differentiation
- TESPSA reduces bacterial adhesion and biofilm formation
- TESPSA is a promising anchoring platform of biomolecules onto titanium

1. Introduction

Commercially pure titanium is the material of choice for dental implants because of its excellent corrosion resistance, mechanical strength and biocompatibility. Nevertheless, lack of osseointegration during early healing or infection of the peri-implant tissues can lead to bone resorption and device failure. Therefore, the success of dental implants requires not only an optimum osseointegration or the development of a soft tissue seal around the transmucosal part of the implant, but also the contribution of some antibacterial properties to the metallic substrate.

When an implant is placed in the oral cavity it is immediately exposed to microorganism colonization, triggering a biofilm formation [1]. First colonizers (such as S*treptococcus sanguinis*) are a required step of this process due to their role in the early attachment and guidance of later colonizers [2, 3]. In addition, other species, such as *Lactobacillus salivarius*, can associate with other colonizers and their by-products are important for the biofilm formation and maintenance [3].

The success of an implant is related with the 'race to the surface' between microbial adhesion and biofilm growth vs. cell adhesion and tissue integration. If the race is won by cells, then the surface is covered by tissue and is less vulnerable to bacterial colonization. If the race is won by bacteria, however, the implant surface is rapidly covered by a biofilm and tissue cell functions are impaired by bacterial virulence factors and toxins [4, 5].

Current strategies for improving the success of implants have been focused on the improvement of osseointegration through osteoinduction and hence preventing biofilm formation on implant surfaces. Development of titanium coatings using bioactive molecules are expected to optimize the biological response to the implants by stimulation of osteoblast maturation and minimization of bacterial adhesion [6]. Bioactive molecules can be covalently attached to surfaces with self-assembled monolayers based on silanes, siloxanes, phosphoric

acid or thiols [7]. In the case of silanization, silane molecules act as a binder between the substrate and the biomolecules. This technique could be improved using silanes that elicit specific cell responses, such as proliferation, differentiation [8] or antibacterial effects [9,10].

The present work aimed to reduce biofilm formation and enhance osseointegration on dental implants by incorporating the silane triethoxysilylpropyl succinic anhydride (TESPSA) as a functional molecule to titanium surfaces. *In vitro* proliferation and differentiation rates of osteoblast and fibroblast cells on TESPSA-treated titanium surfaces were measured. Antibacterial properties of the silanized surfaces were studied against primary and late bacteria colonizers of the oral biofilm. An *in vitro* cell-bacteria co-culture was also performed to analyze the interaction between bacteria and fibroblast cells.

2. Materials and methods

2.1. Sample preparation

Grade 2 titanium disks (10 mm diameter, 2 mm thickness) were polished and sonicated in isopropanol, ethanol, distilled water and acetone for 15 minutes each. These samples are referred to as 'Ti', and were used as control group.

Polished titanium surfaces were activated by alkaline etching with 5M NaOH for 24 h at 60ºC as previously described [11,12]. These samples are referred to as 'Ti_N'.

Activated titanium surfaces were silanized with TESPSA with a method adapted, with some modifications, from previously published protocols [13,14]. Briefly, titanium samples were immersed in 0.5 % (v/v) TESPSA in anhydrous toluene for 1 h at 70ºC in nitrogen atmosphere. 3% (v/v) of N,N-diisopropylethylamine (DIEA) was added in order to keep a basic environment. Once treated, samples were sonicated 10 minutes in toluene, washed with isopropanol, ethanol, distilled water and acetone, and dried with nitrogen. These samples are referred to as 'Ti_TSP'.

2.2. Physico-chemical characterization

Scanning electron microscopy (SEM) (Zeiss Neon40 FE-SEM, *Carl Zeiss* NTS GmbH, Germany) was used to analyze the surface morphology of the surfaces. For each sample, five images were taken at a working distance of 7 mm and a potential of 5 kV.

A white-light optical profiling system (Wyko NT1100, Veeco Instruments, USA) was used to evaluate the surface roughness. A vertical scanning interferometry mode was used with a 5× objective, resulting in a scanning area of 736x480 µm. Data analysis was performed with Wyko Vision 232^{TM} software (Veeco Instruments). The roughness parameters computed were the arithmetic average height (R_a), the surface skewness (R_{sk}), and the surface kurtosis (R_{ku}). For each condition, three samples were evaluated with three measurements per sample.

The sessile drop method was used to determine the hidrophilicity of the surfaces by a Contact Angle System (OCA15 plus, Dataphysics, Germany). The drop volume was 3 µl with a dosing rate of 1 $\mu l \cdot min^{-1}$. Ultrapure distilled water (Millipore Milli-Q, Merck Millipore Corporation, USA) and diiodomethane (Sigma-Aldrich, Spain) were used as working fluids. Three measurements were carried out for three different samples in each series. All measurements were performed at room temperature. Data was analyzed with the SCA 20 software (Dataphysics). Determination of surface free energy was calculated with the Owens and Wendt equation [15].

X-ray photoelectron spectroscopy (XPS) was used to analyze the surface chemical composition. XPS samples spectra were acquired with an XR50 Mg anode source operating at 150W and a Phoibos 150 MCD-9 detector (D8 advance, SPECS Surface Nano Analysis GmbH, Germany). High resolution spectra were recorded with pass energy of 25 eV at 0.1 eV steps and a pressure below $7.5 \cdot 10^{-9}$ mbar. Binding energies were referred to the C 1s signal. Two samples were studied for each working condition.

2.3. In vitro cell assays

Human primary foreskin fibroblasts (HFFs; Merck Millipore Corporation, Bedford, MA, USA) and Sarcoma osteogenic osteoblast-like cell line (SaOS-2; ATCC, Manassas,VA, USA) were cultured in Dulbecco's Modified Eagle Medium (DMEM) and McCoy's medium modified, respectively. Both mediums were supplemented with 10% fetal bovine serum (FBS), 2 mM L-glutamine and penicillin/streptomycin (50 $U \cdot ml^{-1}$, 50 $\mu g \cdot ml^{-1}$ respectively) (all reagents from Invitrogen, Carlsbad, CA, USA) at 37ºC and 5% CO_2 in a humidified incubator, renewed every 2 days. HFFs at passage eight and osteoblast-like cells at passage twenty nine were used in all experiments.

2.3.1. Proliferation of HFFs and SaOS-2 cells

Cells were seeded onto titanium samples at a density of 5000 cells/disk and incubated at 37ºC. After 4 hours, 1, 3 and 7 days of incubation, cells were lysed with 200 µl/well of M-PER® (Pierce, Rockford, IL, USA). Proliferation of cultured cells on the studied surfaces was determined using the Cytotoxicity Detection Kit LDH (Roche Applied Science, Mannheim, Switzerland) according to the manufacturer's instructions. The release of lactate dehydrogenase (LDH) was measured spectrophotometrically at 492 nm with an ELx800 Universal Microplate Reader (Bio-Tek Instruments, Inc. Winooski, VT, USA). Tissue culture polystyrene (TCPS) was used as control substrate.

2.3.2. Osteoblastic gene expression

Total RNA, at different culture time, was extracted using RNeasy® Mini Kit (Qiagen, Hilden, Germany) as described in the manufacturer's instructions. RNA was quantified using NanoDrop ND-1000 spectrophotometer (NanoDrop Technologies Montchanin, DE, USA). 100 ng were retrotranscribed to cDNA using the QuantiTect Reverse Transcription Kit (Qiagen). cDNA products were diluted to 1 ng μl^{-1} and used as real-time quantitative Polymerase Chain Reaction (RT-qPCR) templates. Primers were selected from the Universal

ProbeLibrary (Roche Applied Science) to amplify specific genes of osteoblast differentiation (Table 1).

Primers from genes that exhibited more than one transcript were selected from common regions. SYBR Green RT-qPCR analyses were carried out using the QuantiTect SYBR Green RT-PCR Kit (Qiagen) in a StepOnePlus real-time PCR machine (Thermo Fisher Scientific, Waltham, MA, USA). Specificity of each RT-qPCR reaction was determined by melting curve analysis.

All samples were normalized by the expression levels of β-actin (reference gene) and fold changes were related to Ti at 4h of culture as follows:

$$FC = E_{target}^{\Delta Cq.target[Ti.4h]} / E_{reference}^{\Delta Cq.reference[Ti.4h]} \quad (1)$$

Where *Cq* is the median value for the quantification cycle for the triplicate of each sample and *E* is the amplification efficiency, determined from the slope of the log-linear portion of the calibration-curve, as:

$$E = 10^{1/slope} \quad (2)$$

2.4. Bacterial strains and culture conditions

Bacterial assays were done with *Streptococcus sanguinis* (CECT 480; Spanish Culture Collection, Spain) and *Lactobacillus salivarius* (CCUG 17826; Culture Collection University of Göteborg, Sweden). *S. sanguinis* was growth and maintained on Todd-Hewitt (TH) broth (Scharlab SL, Sentmenat, Spain) and *L. salivarius* on MRS broth (Scharlab SL).

Cultures were incubated overnight at 37ºC and the optical density adjusted to 0.2±0.01 units at 600 nm (approx. $1 \cdot 10^8$ colony forming units (CFU)ml^{-1} for each strain) [16].

2.4.1. Bacterial adhesion to treated surfaces

This protocol has been previously described [11,12,16]. Briefly, functionalized and control samples were immersed in 1 ml of bacterial suspensions ($1 \cdot 10^8$ CFU ml^{-1}) for 2 hours at 37ºC. Bacteria were detached by vortexing, diluted and seeded on agar plates. The plates were then incubated at 37ºC for 24 h and the resulting colonies were counted.

2.4.2. Evaluation of biofilm formation onto treated surfaces

This evaluation has been detailed elsewhere [11,12,16]. Samples were immersed in 1 mL of bacterial suspension for 2 h. Next, the medium was replaced by fresh medium and bacteria were allowed to grow for 24 h at 37ºC. Then, 200 µL of BacTiter-Glo Reagent (Promega, Madison, WI, USA) were added to each sample and 15 min later the luminescence was measured (Infinite 200 PRO, Tecan, Männedorf, Switzerland).

2.4.3. Cell-bacteria co-cultures

This protocol was modified from a published study [17]. Treated surfaces and control samples were immersed in *S.sanguinis* and *L.salivarius* strain suspensions (concentration of 10^8 bacteria ml^{-1}) in their corresponding medium and incubated at 37ºC for 2 hours. Next, bacteria suspensions were removed and samples were washed three times in sterile PBS. Then, HFFs cells suspended in modified culture medium (supplemented with 2% of the appropriate bacteria growth medium) were seeded on bacteria-coated surfaces at a density of 25,000 cells/well. Bacteria and HFFs were maintained at 37ºC in humidified 5% CO_2 for 24 and 48 h. At specific times, HFFs cells were fixed, stained with Alexa fluor 546-phalloidin (Invitrogen) and DAPI (Invitrogen) and analyzed. The outcome of the experiment was expressed as the reduction in surface coverage percentage by HFFs cells in the presence of adhering bacteria compared to bacteria-free samples. All experiments were performed in triplicate for each type of surface.

2.5. Statistical analysis

All data are presented as mean value ± standard deviation. A non-parametric U Mann-Whitney test was used to analyze significant differences in contact angle and roughness measurements. A non-parametric Kruskal-Wallis test was used for the other measurements. Significance level was set at P value < 0.05.

3. Results

3.1. Physico-chemical characterization

Control titanium surfaces (Figure 1a) exhibited a smooth surface, while NaOH treated samples (Figure 1b) revealed a microrough layer of sodium titanate [18]. Silanization with TESPSA did not affect the morphology (data not shown). The layer observed on NaOH treated samples (Ti_N) had an increased surface roughness compared to control surfaces (Ti) (Table 2). The silanization with TESPSA (Ti_N_TSP) had no effect on roughness parameter compared to activated samples (Ti_N).

The activation with NaOH significantly reduced the wettability of the surface, increasing the surface free energy (SFE) (Table 3). The silanization process using TESPSA yielded a minor increase in the contact angle values and a slight decrease in SFE in comparison with Ti_N samples. Throughout the process of silanization, the changes observed in SFE were due to variation in its polar part. Statistically significant differences were noticed for all wettability parameters between control Ti, Ti_N and TI_N_TSP.

Smooth titanium presented a surface chemical composition of approximately 45% C, 1% N, 40% O and 12% Ti (Table 4). Activation of titanium samples with NaOH resulted in a significant decrease in carbon presence, but also in an increase in oxygen content and the presence of sodium in the sample (4.7%) suggesting the existence of a sodium titanate layer on the surface [19]. After TESPSA silanization, the presence of silicon was detected,

corresponding to the presence of silanes on the surface. Deconvolution of high resolution spectra of C 1s and O 1s peaks detected an increase in the presence of Ti-OH and C-C species (Table 5).

3.2. In vitro assays

3.2.1. Proliferation and cell viability

After 3 days of incubation, HFFs cell count results showed significant differences in the number of viable cells in titanium samples vs control TCPS (Figure 2a). At 7 days of cell culture, cell numbers for Ti_N and Ti_N_TSP remained significantly lower than those of control Ti and TCPS, but the reduction was not lower than the limit of 20% signaling possible cytotoxic effects.

For osteoblast-like SaOS-2 cells, treated samples (Ti_N and Ti_N_TSP) showed less cells than control surfaces (Ti and TCPS) at day 1 (Figure 2b). Over time, however, cell count converged, with no significant differences between groups after 7 days except for TCPS.

3.2.2. Osteoblastic gene expression

RUNX2 gene expression was highly upregulated at 4 hours, but only on Ti_N_TSP samples (Figure 3a). One of the target genes of RUNX2 is collagen I alpha 1 (COL1A1). Ti_N highly stimulated COL1A1 gene expression at 4 hours, followed by a slow reduction with time, but only a slightly increased expression on day 1 was detected for Ti and Ti_N_TSP (Figure 3b).

ALP gene expression exhibited the highest values at 4 hours on Ti_N and Ti_N_TSP surfaces (Figure 3c). Silanized samples also showed significantly higher ALP expression values compared to the other surfaces after 1 and 3 days.

The expression of BMP-2 was also evaluated as an indicator of osteoblast activity. The gene expression level of BMP-2 highly increased for TESPSA treated surfaces (Figure 3d).

3.2.3. Bacterial adhesion and biofilm formation on titanium surfaces

Bacterial adhesion (Figure 4) and biofilm formation (Figure 5) reduced significantly for both *S.sanguinis* and *L.salivarius* strains on silanized surfaces.

3.2.4. Cell-bacteria co-cultures

The presence of either bacteria strain reduced the coverage of HFFs cells on control surfaces and NaOH-treated surfaces after 24 and 48h of growth. On Ti_N_TSP, however, HFFs cell coverage significantly increased even in the presence of bacteria (Figure 6).

Cell adhesion and spreading, too, was much higher for silanized samples than for the other two studied surfaces, where some cells stayed rounded even after 24 and 48 h (Figure 7). Interestingly, HFFs cells showed maximum spreading in the absence of bacteria as well as on silanized samples immersed in co-culture suspension.

4. Discussion

The success of an implanted biomaterial depends, among other factors, on the outcome of the 'race for the surface' between tissue cells and bacterial biofilm growth [20]. Bacterial infection may delay osseointegration, compromising tissue cell functions and even leading to implant failure [21]. A surface with antibacterial properties, high capacity for cell attachment and able to release biological factors could be an effective way to avoid bacteria adhesion and improve osseointegration. Previous studies had suggested that different silanes could affect osteoblasts [8] or present antibacterial activity on steel, Ti6Al4V or glass [9,10]. This study tested *in vitro* the hypothesis that titanium coated with TESPSA silane has antibacterial properties while inducing osteoblast differentiation. Particularly, Godoy-Gallardo *et al*. [11,12,22] explored the use of two distinct silanes, APTES and CPTES, in order to covalently immobilize an antibacterial peptide onto titanium surface. The results showed antibacterial properties only in presence of the peptide. The results suggested that APTES and CPTES are

not able to provide antibacterial or antifouling properties to titanium. Thus, the strategy reported in this work holds great promise for further clinical development due to the reduction of bacterial adhesion and biofilm formation without any antibacterial peptide.

In order to improve TESPSA attachment on titanium, the samples were first activated with a solution of NaOH to increase the number of available hydroxyl groups on the surface [23]. A stable amorphous sodium titanate layer was formed on the surface of the activated samples [18, 19] with a characteristic nanomorphology (Figure 1b) and increased surface roughness (Table 2).

NaOH activation modified the surface roughness at the nanoscale level (Table 2). Early adhesion of osteoblasts decreased (Figure 2b) but not of fibroblasts (Figure 2a), in agreement with other studies [24,25]. The roughness increase on Ti_N samples, however, did not significantly affect RUNX2 expression, a factor linked to cell differentiation (Figure 3a).

Bacterial colonization is also influenced by surface roughness. The NaOH treatment slightly increased bacterial adhesion without affecting biofilm formation. These results are in accordance with those of Montanaro *et al*, which suggested an increase of bacterial adhesion for mean roughness values over 155 nm [26].

Cell and bacteria adhesion behavior is linked to wettabililty and SFE, too [27-29]. This influence is mainly due to the presence of hydrophilic or hydrophobic chemical groups of the surface. As shown in Table 3, the activation treatment induced a substantial decrease in contact angle values, related to the cleaning effect and the formation of hydroxyl groups [30]. The combined generation of roughness and hydrophilicity after NaOH treatment produced a suitable surface for silane immobilization. The main causes are the increase of real surface area, the removal of surface contaminants and the generation of hydroxyl groups on the surface that increase the probability of interactions between the activated surface and the ethoxy groups of the silane [11,31,32]. Ti_N_TSP contact angle values, however, increased

compared to Ti_N due to the hydrophobic behavior of the silane. These results are corroborated with other studies which activated titanium surface using the same strategy [11,12,22].

The efficiency of TESPSA silanization was determined using XPS analysis (Table 4 and Figure 1S (Supplementary Information)). Untreated surfaces presented three C 1s peaks (284.8, 285.7 and 288.1 eV, Table 5) associated to hydrocarbon contamination (CHx, C-O and C=O bonds) [33-35]. After NaOH activation, total carbon presence was lower, and C 1s high resolution spectra was fitted to two peaks at 284.8 and 288.8 eV which can be attributed to C-H and C=O respectively [33-35]. These results indicate that Ti_N surfaces were cleaner after the NaOH treatment. Besides, sodium was detected after NaOH activation due to the formation of a sodium titanate layer [18,19] as has been showed in SEM micrographs (Figure 1). After TESPSA immobilization, presence of silicon (6.9%) and an increase of C 1s peak at 284.6 eV (assigned to C-C) were measured. These results can be attributed to the presence of the silane. The peak linked to the Si-O bond (Table 5) remained after sonication, as expected for silane molecules chemically bonded to the titanium surface [36].

Once the bonding of the silane to the titanium surface was established, the potential effect of TESPSA on osteoblast differentiation was studied through gene expression of osteoblast markers. Osteoblast differentiation is a finely regulated process in which the expression of several genes is highly controlled [37-39]. In this scenario, the transcription factor RUNX2 plays an essential role since it binds and regulates the expression of multiple genes expressed in osteoblasts [40]. The presence of TESPSA on titanium surface highly increased RUNX2 gene expression at 4h of culture but not afterwards, suggesting an early increase in osteoblast activity (Figure 3a).

One of the target genes of RUNX2 is COL1A1, which is an indicator of the transition between pre-osteoblast and immature osteoblast, suggesting that cells are probably in the

mature state [41]. The present results showed a slight increase in COL1A1 expression after 24h of culture when TESPSA is immobilized, without significant differences compared to titanium (Figure 3b).

The expression of BMP-2 was also evaluated as an indicator of osteoblast activity because it induces osteoblast differentiation [42]. The results exhibit remarkably higher osteoblast activation in the presence of TESPSA, since the gene expression level of BMP-2 increased more than a hundredfold at all measured times (Figure 3c). These results suggest that TESPSA immobilization on titanium has osteoinductive effects without the need of any biomolecule, avoiding the problems related to biomolecule degradation [7].

Samples with TESPSA displayed a reduction in bacterial adhesion (Figure 4) and biofilm formation (Figure 5) for both *S.sanguinis* and *L.salivarius*. Even so, the two bacterial strains used in this study display different sensitivities to the activity of TESPSA-silanized surfaces. More studies should be conducted to better elucidate the causes of such behavior.

A cell-bacteria co-culture study was also performed because it provides a better mimic of the clinical situation than mono-cultures studies with either bacteria or cells [4, 17]. The outcome of co-culture studies involving bacteria and tissue cells depends on a multitude of factors [4, 5]. The presence of bacteria affects both cell attachment and spreading on Ti and Ti_N surfaces (Figure 7). It is noticeable, however, that HFFs spread equally well on TESPSA-treated surfaces in the presence of bacteria than in bacteria-free cultures.

The *in vitro* effects of TESPSA-treated titanium surfaces are the expected for a surface with antibacterial properties that avoids or delays bacteria adhesion and enhances cell adhesion and spreading. Surfaces treated with TESPSA could enhance the biological sealing on dental implant surfaces against bacteria colonization of underlying tissues. Furthermore, it can be an effective anchoring platform of biomolecules on titanium surfaces with improved osteoblast differentiation and antibacterial properties. Further work in this direction should include

antibacterial assays using complete multispecies models of oral biofilm that more realistically mimic the complex biology involved in peri-implantitis.

5. Conclusions

A TESPSA silane was attached to titanium surfaces and evaluated *in vitro*. No cytotoxic effects were observed against HFFs and osteoblast-like SaOS-2 cells. TESPSA-treated surfaces increased the expression of osteoblastic cell differentiation markers. A noticeable reduction in the adhesion and early stages of biofilm formation of *S.sanguinis* and *L.salivarius* was observed. Cell adhesion and spreading in cell-bacteria co-cultures on titanium surfaces treated with TESPSA showed similar results to cell cultures without bacteria presence.

TESPSA immobilization on titanium is a promising strategy to generate antibacterial and osteoinductive titanium surfaces.

Acknowledgements

This work was supported by Fundación Ramón Areces and the Spanish Government (MINECO) under Grants MAT2009-12547 and MAT2012-30706, both co-funded by the European Union through European Regional Development Funds.

M. Godoy-Gallardo and F.J. Gil report that they have a patent (ES patent P201 331756) on the TESPSA silane application.

References

1. Wang Z, Shen Y, Haapasalo M. Dental materials with antibiofilm properties. Dent Mater 2014;30:e1–e16.
2. Mayanagi G, Sato T, Shimauchi H, Takahashi N. Microflora profiling of subgingival and supragingival plaque of healthy and periodontitis subjects by nested PCR. Int Congr Ser 2005;1284:195–6.

3. Pham LC, van Spanning RJM, Röling WFM, Prosperi AC, Terefework Z, Ten Cate JM, Crielaard W, Zaura E. Effects of probiotic *Lactobacillus salivarius* W24 on the compositional stability of oral microbial communities. Arch Oral Biol 2009;54:132–7.
4. Subbiahdoss G, Kuijer R, Grijpma DW, van der Mei HC, Busscher HJ. Microbial biofilm growth vs. tissue integration: 'the race for the surface' experimentally studied. Acta Biomater 2009;5:1399–404.
5. Subbiahdoss G, Grijpma DW, van der Mei HC, Busscher HJ, Kuijer R. Microbial biofilm growth versus tissue integration on biomaterials with different wettabilities and a polymer-brush coating. J Biomed Mater Res A 2010;94A:533–8.
6. Norowski PA Jr, Bumgardner JD. Biomaterial and antibiotic strategies for peri-implantitis: a review. J Biomed Mater Res B Appl Biomater 2009;88:530–43.
7. Bauer S, Schmuki P, von der Mark K, Park J. Engineering biocompatible implant surfaces: Part I: Materials and surfaces. Prog Mater Sci 2013;58:261–326.
8. Toworfe GK, Bhattacharyya S, Composto RJ, Adams CS, Shapiro IM, Ducheyne P. Effect of functional end groups of silane self-assembled monolayer surfaces on apatite formation, fibronectin adsorption and osteoblast cell function. J Tissue Eng Regen Med 2009;3:26-36.
9. Ma Y, Chen M, Jones JE, Ritts AC, Yu Q, Sun H. Inhibition of *Staphylococcus epidermidis* biofilm by trimethylsilane plasma coating. Antimicrob Agents Chemother 2012;56:5923-37.
10. Katsikogianni MG, Missirlis YF. Interactions of bacteria with specific biomaterial surface chemistries under flow conditions. Acta Biomater 2010;6:1107-18.
11. Godoy-Gallardo M, Mas-Moruno C, Fernández-Calderón MC, Pérez-Giraldo C, Manero JM, Albericio F, Gil FJ, Rodríguez D. Covalent immobilization of hLf1-11 peptide on a titanium surface reduces bacterial adhesion and biofilm formation. Acta Biomater 2014;10:3522-34.
12. Godoy-Gallardo M, Mas-Moruno C,Yu K, Manero JM, Gil FJ, Kizhakkedathu JN, Rodriguez D. Antibacterial properties of hLf1–11 peptide onto titanium surfaces: a comparison study between silanization and surface initiated polymerization.Biomacromolecules 2014;16:483-96.

13. Xiao SJ, Textor M, Spencer ND, Wieland M, Keller B, Sigrist H. Immobilization of the cell-adhesive peptide Arg-Gly-Asp-Cys (RGDC) on titanium surfaces by covalent chemical attachment. J Mater Sci Mater Med 1997;8:867–72.
14. Chen X, Sevilla P, Aparicio C. Surface biofunctionalization by covalent co-immobilization of oligopeptides. Colloids Surf B Biointerfaces 2013;107:189–97.
15. Owens DK, Wendt RC. Estimation of the surface free energy of polymers. J Appl Polym Sci 1969;13:1741–7.
16. Godoy-Gallardo M, Rodríguez-Hernández AG, Delgado LM, Manero JM, Javier Gil F, Rodríguez D. Silver deposition on titanium surface by electrochemical anodizing process reduces bacterial adhesion of *Streptococcus sanguinis* and *Lactobacillus salivarius*. Clin Oral Implants Res 2014; DOI:10.1111/clr.12422.
17. Zhao B, van der Mei HC, Subbiahdoss G, de Vries J, Rustema-Abbing M, Kuijer R, Busscher HJ, Ren Y. Soft tissue integration versus early biofilm formation on different dental implant materials. Dent Mater 2014;30:716–27.
18. Kim HM, Miyaji F, Kokubo T, Nakamura T. Effect of heat treatment on apatite-forming ability of Ti metal induced by alkali treatment. J Mater Sci Mater Med 1997;8:341–7.
19. Aparicio C, Padrós A, Gil F-J. In vivo evaluation of micro-rough and bioactive titanium dental implants using histomorphometry and pull-out tests. J Mech Behav Biomed Mater 2011;4:1672–82.
20. Gristina AG. Biomaterial-centered infection: microbial adhesion versus tissue integration. Science 1987;237:1588–95.
21. Gulati K, Ramakrishnan S, Aw MS, Atkins GJ, Findlay DM, Losic D. Biocompatible polymer coating of titania nanotube arrays for improved drug elution and osteoblast adhesion. Acta Biomater 2012;8:449–56.
22. Godoy-Gallardo M, Wang Z, Shen Y, Manero J.M, Gil F.J, Rodriguez D, Haapasalo M. Antibacterial coatings on titanium surfaces: a comparison study between in vitro single-species and multispecies biofilm. ACS Appl Mater Interfaces 2015;7(10):5992-6001
23. Han Y, Mayer D, Offenhäusser A, Ingebrandt S. Surface activation of thin silicon oxides by wet cleaning and silanization. Thin Solid Films 2006;510:175–80.

24. Kieswetter K, Schwartz Z, Hummert TW, Cochran DL, Simpson J, Dean DD, Boyan BD. Surface roughness modulates the local production of growth factors and cytokines by osteoblast-like MG-63 cells. J Biomed Mater Res 1996;32:55–63.

25. Raines AL, Olivares-Navarrete R, Wieland M, Cochran DL, Schwartz Z, Boyan BD. Regulation of angiogenesis during osseointegration by titanium surface microstructure and energy. Biomaterials 2010;31:4909–17.

26. Montanaro L, Campoccia D, Arciola CR. Advancements in molecular epidemiology of implant infections and future perspectives. Biomaterials 2007;28:5155–68.

27. Grivet M, Morrier JJ, Benay G, Barsotti O. Effect of hydrophobicity on in vitro streptococcal adhesion to dental alloys. J Mater Sci Mater Med 2000;11:637–42.

28. Strevett KA, Chen G. Microbial surface thermodynamics and applications. Res Microbiol 2003;154:329–35.

29. Harnett EM, Alderman J, Wood T. The surface energy of various biomaterials coated with adhesion molecules used in cell culture. Colloids Surf B Biointerfaces 2007;55:90–7.

30. Barbour ME, O'Sullivan DJ, Jenkinson HF, Jagger DC. The effects of polishing methods on surface morphology, roughness and bacterial colonisation of titanium abutments. J Mater Sci Mater Med 2007;18:1439–47.

31. Barabanova AI, Pryakhina TA, Afanas'ev ES, Zavin BG, Vygodskii YS, Askadskii AA, Philippova OE, Khokhlov AR. Anhydride modified silica nanoparticles: Preparation and characterization. Appl Surf Sci 2012;258:3168–72.

32. Cras JJ, Rowe-Taitt CA, Nivens DA, Ligler FS. Comparison of chemical cleaning methods of glass in preparation for silanization. Biosens Bioelectron 1999;14:683–8.

33. Martin HJ, Schulz KH, Bumgardner JD, Walters KB. An XPS study on the attachment of triethoxsilylbutyraldehyde to two titanium surfaces as a way to bond chitosan. Appl Surf Sci 2008;254:4599–605.

34. Song Y-Y, Hildebrand H, Schmuki P. Optimized monolayer grafting of 3-aminopropyl triethoxysilane onto amorphous, anatase and rutile TiO_2. Surf Sci 2010;604:346–53.

35. Tan G, Zhang L, Ning C, Liu X, Liao J. Preparation and characterization of APTES films on modification titanium by SAMs. Thin Solid Films 2011;519:4997–5001.

36. Howarter JA, Youngblood JP. Optimization of silica silanization by 3-aminopropyl triethoxysilane. Langmuir 2006;22:11142–7.

37. Rodan GA, Noda M. Gene expression in osteoblastic cells. Crit Rev Eukaryot Gene Expr 1991;1:85–98.

38. Perinpanayagam H, Martin T, Mithal V, Dahman M, Marzec N, Lampasso J, Dziak R. Alveolar bone osteoblast differentiation and Runx2/Cbfa1 expression. Arch Oral Biol 2006;51:406–15.

39. Sista S, Wen C, Hodgson PD, Pande G. Expression of cell adhesion and differentiation related genes in MC3T3 osteoblasts plated on titanium alloys: role of surface properties. Mater Sci Eng C 2013;33:1573–82.

40. Lian JB, Stein JL, Stein GS, van Wijnen AJ, Montecino M, Javed A, Gutierrez S, Shen J, Zaidi SK, Drissi H. Runx2/Cbfa1 functions: diverse regulation of gene transcription by chromatin remodeling and co-regulatory protein interactions. Connect Tissue Res 2003;44 Suppl 1:141–8.

41. Aubin JE, Triffitt JT. Mesenchymal stem cells and osteoblast differentiation. In: Bilezikian J, Raisz L, Rodan G, editors. Principles of Bone Biology, 2nd ed. New York: Academic Press; 1996. p 59-81.

42. Yamaguchi A, Ishizuya T, Kintou N, Wada Y, Katagiri T, Wozney JM, Rosen V, Yoshiki S. Effects of BMP-2, BMP-4, and BMP-6 on osteoblastic differentiation of bone marrow-derived stromal cell lines, ST2 MC3T3-G2/PA6. Biochem Biophys Res Commun 1996;220:366–71.

Table 1. DNA sequences of forward (fw) and reverse (rv) primers for the selected genes used for real-time qPCR

Gene symbol	Gene title	Acc. Number	Primer sequence (5'_3')	Amplicon size (bp)
ACTB	Actin, beta	NM_001101.3	fw: AGAGCTACGAGCTGCCTGAC rv: CGTGGATGCCACAGGACT	114
COL1A1	Collagen, type 1, alpha 1	NM_000088.3	fw: AGGTCCCCCTGGAAAGAA rv: AATCCTCGAGCACCCTGA	96
ALP	Alkaline phosphatase, liver/bone/kidney	NM_005245818.1 NM_001127501.2 NM_001177520.1	fw: AGAACCCCAAAGGCTTCTTC rv: CTTGGCTTTTCCTTCATGGT	74
RUNX2	Runt-related transcription factor 2	NM_001024630.3 NM_001015051.3	fw: CGGAATGCCTCTGCTGTTAT rv: TGGGGAGGATTTGTGAAGAC	122
BMP2	Bone morphogenetic protein 2	NM_001200.2	fw: CAGACCACCGGTTGGAGA rv: CCCACTCGTTTCTGGTAGTTCT	95

Table 2. Roughness values (mean ± standard deviation (SD)) for each surface treatment. Statistically significant differences versus control samples (Ti) are indicated with an asterisk ($P < 0.05$).

	R_a [nm]	R_{ku} [nm]	R_{sk} [nm]
Ti	26.0 ± 7.3	6.4 ± 2.0	0.9 ± 0.6
Ti_N	109.0 ± 11.0*	7.4 ± 5.6	0.3 ± 0.5*
Ti_N_TSP	96.9 ± 6.2*	7.5 ± 2.6	0.4 ± 0.8*

Table 3. Values of contact angle (CA), surface free energy (SFE), and its dispersive (DISP) and polar (POL) components, for each surface treatment. Statistically significant differences marked as (a) versus control Ti and as (b) vs Ti_N ($P < 0.05$).

	CA(º)	SFE (mJ/m^2)	DISP (mJ/m^2)	POL (mJ/m^2)
Ti	73.5 ± 7.2	40.8 ± 9.8	34.9 ± 3.3	7.5 ± 3.4
Ti_N	23.6 ± 4.1 [a]	76.6 ± 1.5 [a]	50.4 ± 0.2 [a]	26.2 ± 1.5 [a]
Ti_N_T	31.2 ± 4.6 [a,b]	71.8 ± 2.1 [a,b]	47.3 ± 1.1 [a,b]	24.5 ± 2.2 [a,b]

Table 4. Surfaces' chemical composition (at %). NA: Not assessed.

	C 1s	N 1s	Na 1s	O 1s	Si 2p	Ti 2p
Ti	46.1 ± 6.0	1.1 ± 0.5	NA	40.7 ± 4.8	NA	12.2 ± 1.7
Ti_N	23.1 ± 1.1	1.6 ± 0.5	4.7 ± 0.4	54.2 ± 0.1	NA	16.4 ± 0.2
Ti_N_T	41.2 ± 9.0	0.7 ± 0.2	NA	42.7 ± 6.5	6.9 ± 1.6	8.4 ± 4.1

Table 5. Deconvolution of XPS high resolution spectra: binding energies (eV) and relative intensities (%) of O 1s and C 1s species for each surface treatment.

	Bond State	Position (eV)	% O 1S	Bond State	Position (eV)	% C 1S
Ti	TiO_2	529.9 ± 0.1	46.4 ± 5.8	C-H_X	284.8 ± 0.1	79.6 ± 5.3
	Ti-OH/C=O	531.8 ± 0.2	53.6 ± 5.8	C-O	285.7 ± 0.4	20.3 ± 0.1
				C=O	288.1 ± 0.8	10.3 ± 6.8
Ti_N	TiO_2	529.7 ± 0.1	77.4 ± 3.1	C-H_X	284.8 ± 0.1	79.6± 1.5
	Ti-OH/C=O	531.5 ± 0.2	22.6 ± 3.1	C=O	288.8 ± 0.1	20.4 ± 1.5
Ti_N_TSP	TiO_2/Si-OH	529.7 ± 0.1	39.5 ± 14.4	C-H_X /C-C	284.6 ± 0.1	91.2 ± 1.3
	Ti-OH/ Ti-O-Si/COO	531.5 ± 0.1	60.5 ± 14.3	COO	288.3 ±0.1	8.2 ± 1.2

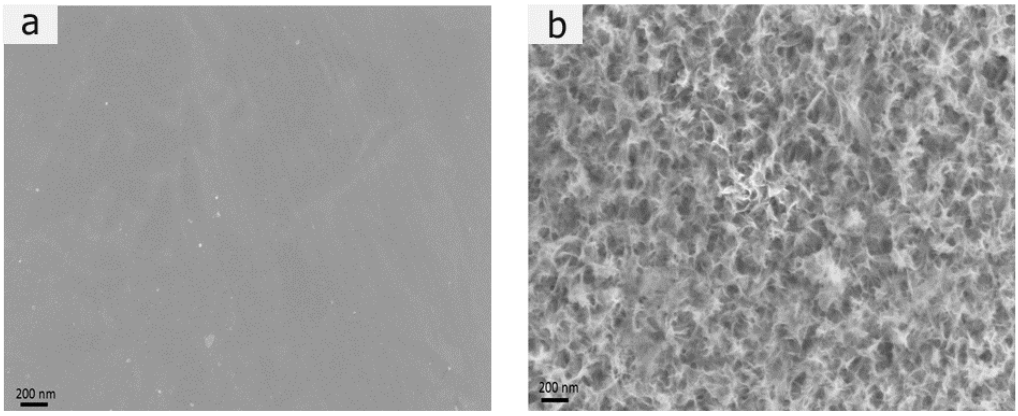

Figure 1. Representative SEM images of the surfaces of: a) smooth titanium (Ti) and b) titanium activated with 5 M NaOH for 24 h at 60ºC (Ti_N).

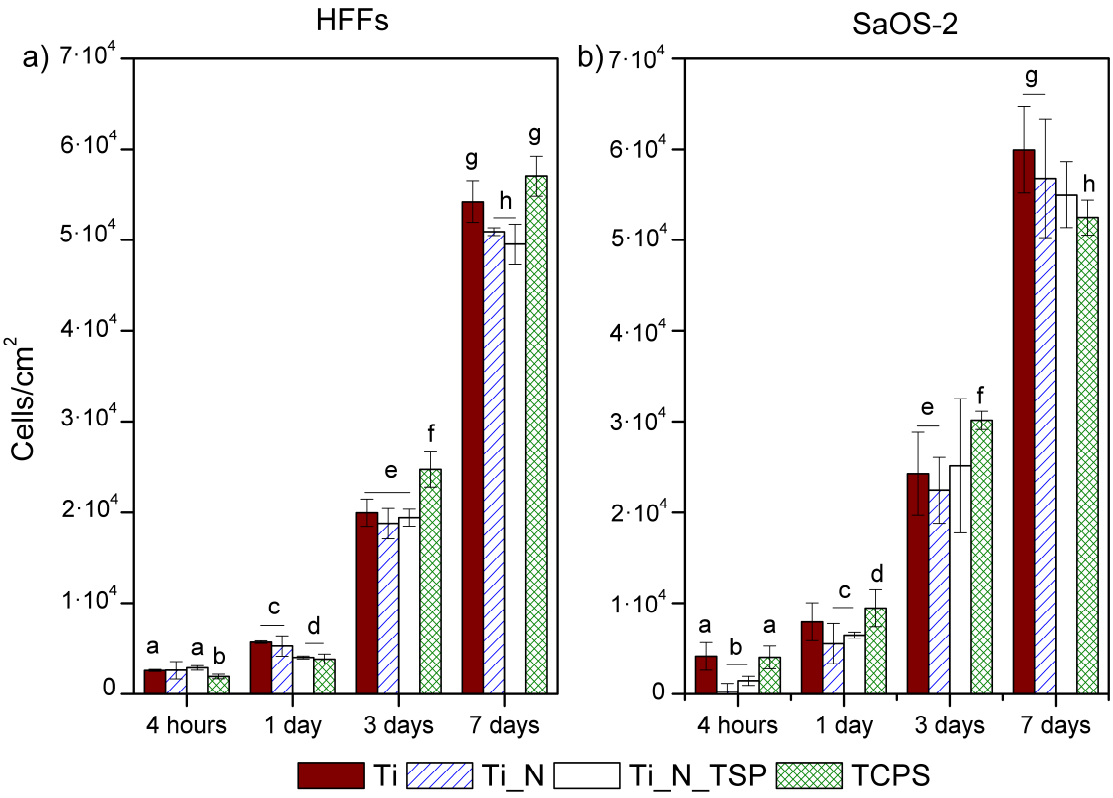

Figure 2. Proliferation of: a) HFFs and b) SaOS-2 onto titanium surfaces after 4 h, 1 day, 3 days and 7 days of incubation. “a” and ”b” indicate significant differences ($P < 0.05$) at 4 hours; “c” and “d” indicate significant differences ($P < 0.05$) at 1 day; “e” and “f” indicate significant differences ($P < 0.05$) at 3 days; “g” and “h” indicate significant differences ($P < 0.05$) at 7 days.

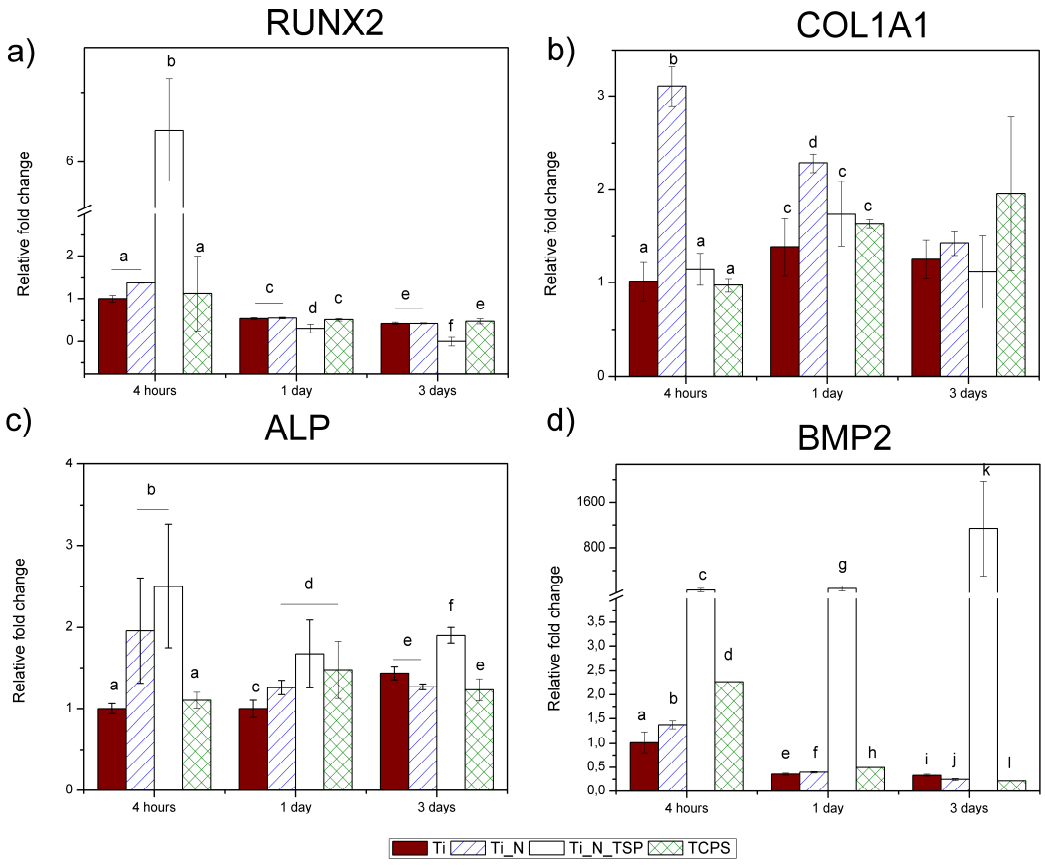

Figure 3. RT-qPCR analyses of the gene expressions of: a) RUNX2, b) COL1A1, c) ALP and d) BMP2, of SaOS-2 cells cultured on the different surfaces at 4, 24 and 72 hours. Results were normalized in respect to expression levels of the endogen reference gene b-actin and are represented as relative fold change to tissue culture polystyrene (TCPS) at 4 h. At each time point, letters indicate significant differences ($P < 0.05$).

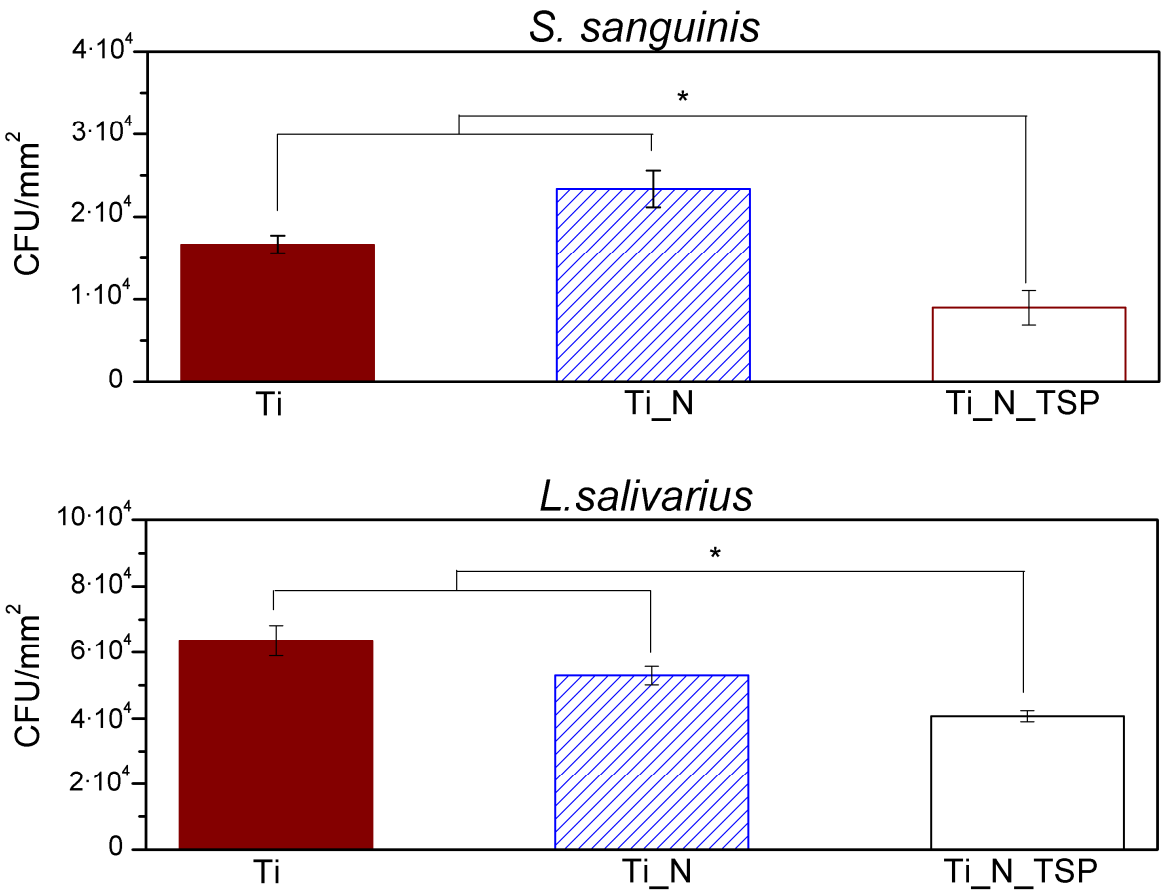

Figure 4. Bacterial adhesion of *S. sanguinis* and *L. salivarius* on titanium surfaces after 2 hours of incubation at 37ºC. Results are displayed as colony-forming units (CFU) normalized vs. the surface area. Statistically significant differences are indicated with "*" ($P < 0.05$).

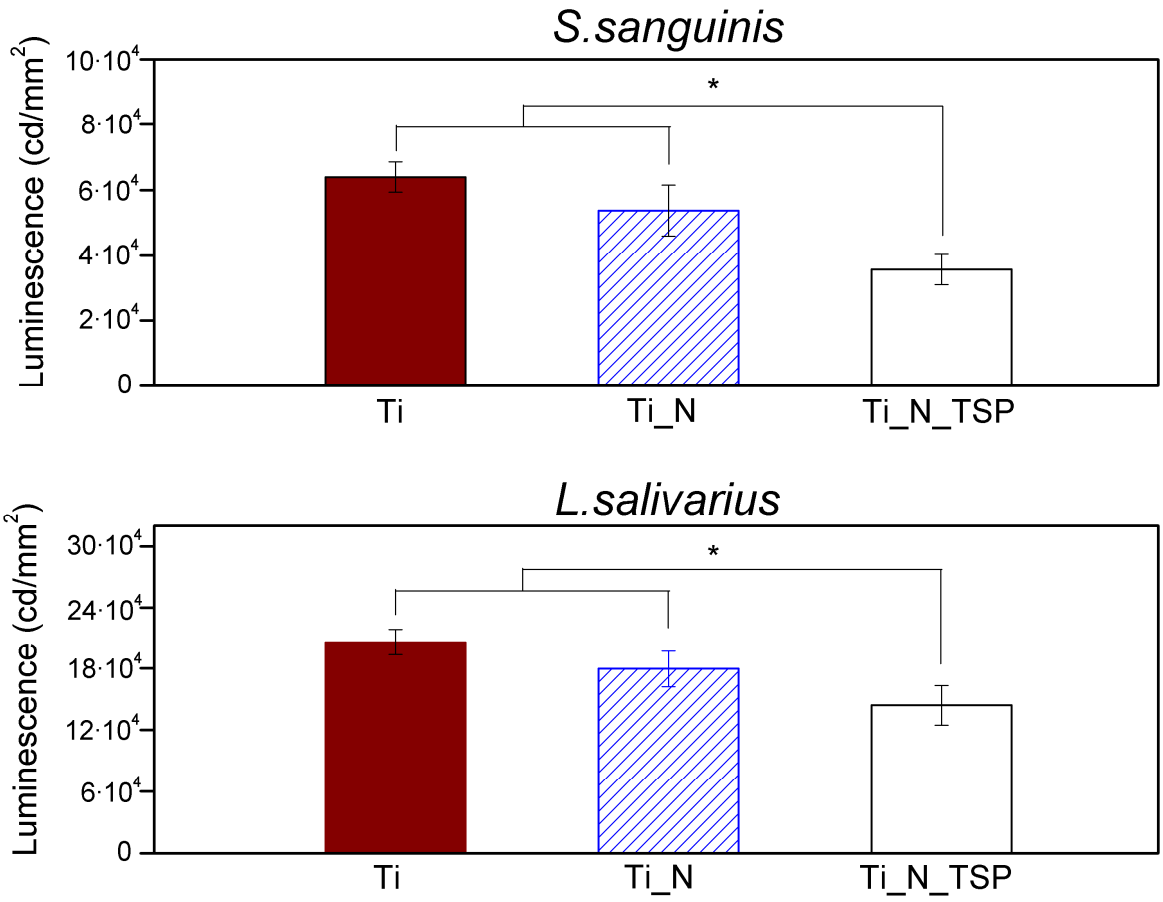

Figure 5. Bacterial biofilm formation of *S. sanguinis* and *L. salivarius* on titanium surfaces after 24 hours of incubation at 37ºC. The metabolically active bacteria are displayed as luminescence intensity (cd) normalized versus the surface area. Statistically significant differences are indicated with "*" ($P < 0.05$).

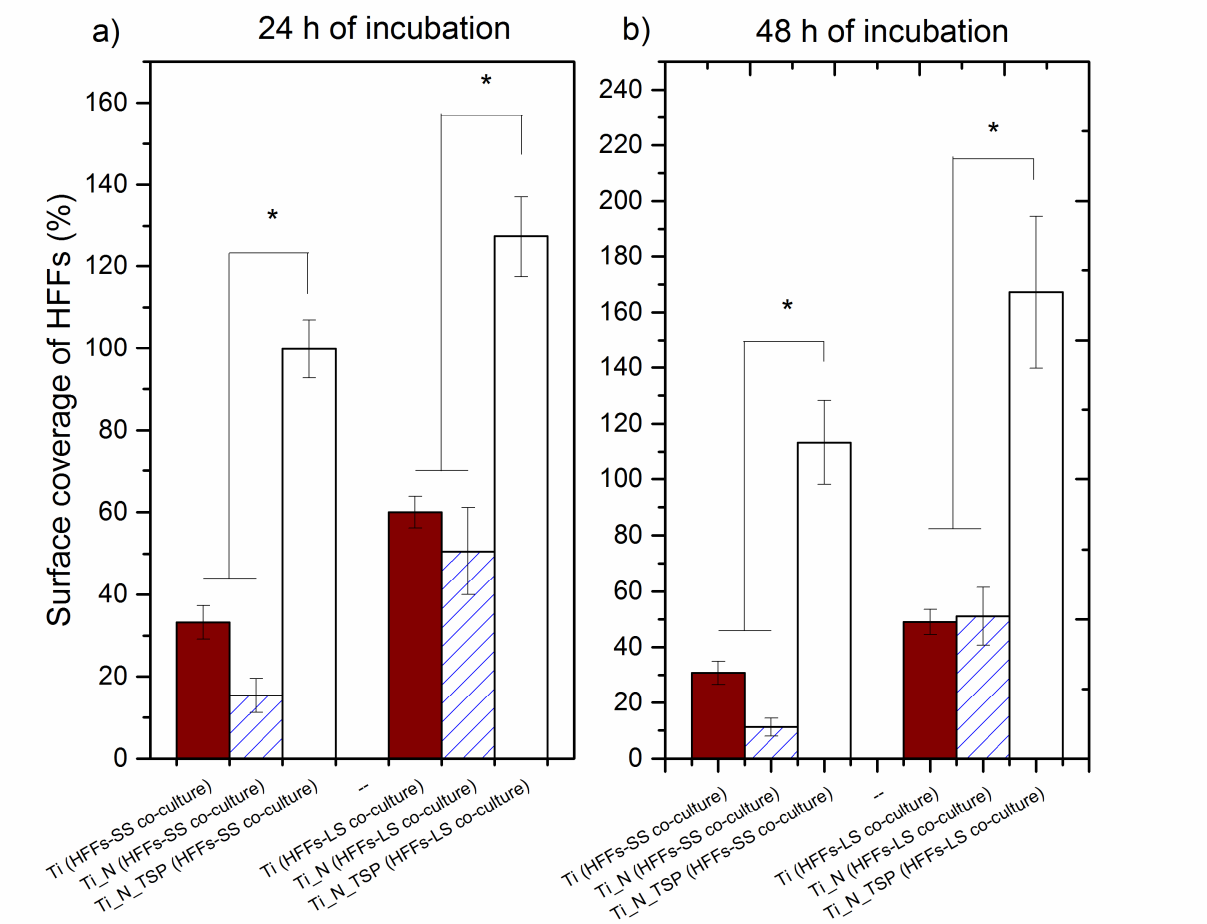

Figure 6. Surface coverage by HFFs and *S.sanguinis* or *L.salivarius* onto treated titanium samples, defined as the number of adhered HFFs cells in the presence of bacteria compared to bacteria-free samples. Error bars indicate standard deviations over triplicate experiments with separately grown cells and bacteria. Statistically significant differences are indicated with "*" ($P < 0.05$).

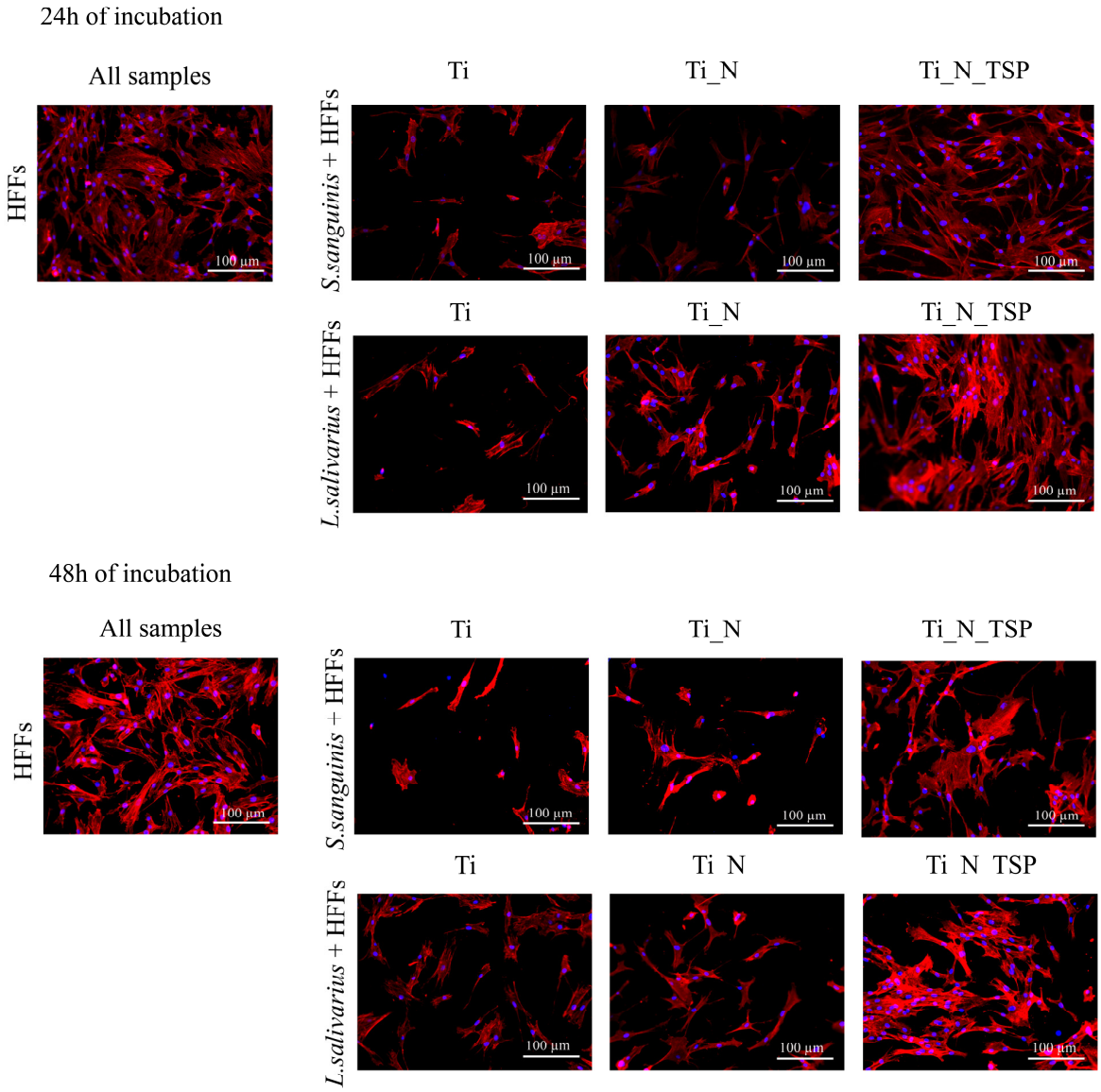

Figure 7. Representative examples of fluorescence images of stained HFFs cells after 24 and 48 h of co-culture growth on the studied surfaces.